IEEE
PHOTONICS
TECHNOLOGY LETTERS

Optical characterization of chalcogenide Ge-Sb-Se waveguides at telecom wavelengths

Molly R. Krogstad, Sungmo Ahn, Wounjhang Park, and Juliet T. Gopinath, *Senior Member, IEEE*

***Abstract*— Nonlinear single-mode $Ge_{28}Sb_{12}Se_{60}$ strip waveguides were demonstrated at 1.53-1.55 μm. The waveguides were fabricated by photo- or e-beam lithography, followed by thermal evaporation and lift-off. The linear propagation loss, ranging from 4.0-6.1 dB/cm, is compared for waveguides under various fabrication conditions. Using measurements of the power-dependent transmission and spectral broadening, the nonlinear loss β and nonlinear refractive index n_2 of the waveguides fabricated with e-beam lithography are determined to be 0.014±0.003 cm/GW and $5 \pm 2 \times 10^{-19}$ m^2/W, respectively, at 1.55 μm. Given the large measured figu e of merit, $n_2/(\beta\lambda) = 2.3 \pm 0.9$, this platform holds promise for nonlinear applications at telecom wavelengths.**

***Index Terms*— Optical planar waveguides, nonlinear optics, amorphous materials.**

I. Introduction

APPLICATIONS such as ultrafast optical switching and frequency comb generation rely on nonlinear optical effects. Chalcogenide glasses, which contain a chalcogen element such as S, Se, or Te covalently bonded to one or more other elements, provide an excellent platform for compact, broadband, low threshold nonlinear optical devices. The glasses have many attractive properties, including high nonlinearities, transparencies up to 20 μm, and low non-linear absorption [1,2]. We focus on the chalcogenide glass $Ge_{28}Sb_{12}Se_{60}$ primarily because of its As-free composition and large band gap of 1.62 eV [3]. Although characterization of bulk Ge-Sb-Se shows excellent nonlinearity at 1550 nm [4], to the best of our knowledge, no work has been reported characterizing or demonstrating the nonlinearity of Ge-Sb-Se waveguides in this regime. To date, studies on Se-based chalcogenide waveguides have characterized only linear optical properties and typically utilize relatively large mode areas [5,6]. In this letter, we characterize both the nonlinear and linear optical properties of sub-micron Ge-Sb-Se waveguides at 1.53-1.55 μm. The waveguides are found to exhibit large nonlinearity and weak nonlinear absorption, holding promise as a new platform for applications such as ultrafast optical switching in this spectral region.

Manuscript received May 31, 2016; revised September 20, 2016. This work was supported in part by NSF grant EECS-1232077, AFOSR grant FA9550-15-1-0506, and from the DARPA SCOUT program through contract number W911NF-15-1-0621 from ARO. M. R. Krogstad was supported by the Department of Defense (DoD) through the National Defense Science & Engineering Graduate Fellowship (NDSEG) Program.

The authors are with the Departments of Physics and Electrical, Computer, and Energy Engineering, University of Colorado, Boulder, CO 80309 USA. (e-mail: molly.krogstad@colorado.edu).

Digital Object Identifier: 10.1109/LPT.2016.2615189

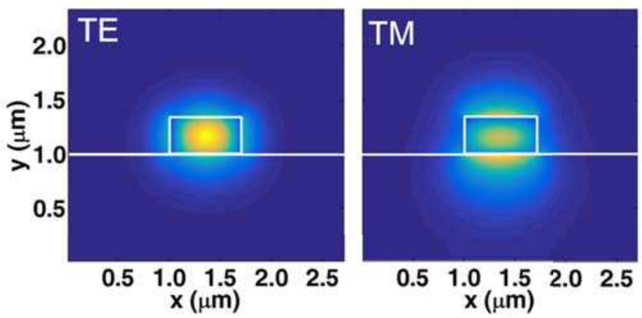

Fig. 1. Simulated TE (left) and TM (right) mode profiles $|E_x|^2$ and $|E_y|^2$ respectively, for the 700 nm by 340 nm Ge-Sb-Se strip waveguides [9]. The white solid outline indicates the x and y position and size of the Ge-Sb-Se core and lower SiO_2 substrate relative to the mode.

II. Waveguide Design and Fabrication

We designed strip, air-clad $Ge_{28}Sb_{12}Se_{60}$ waveguides on a SiO_2 substrate with a range of cross-sectional dimensions, including 2 μm (W) $\times$ 90 nm (H), and 700 nm (W) $\times$ 340 nm (H). The 2 μm $\times$ 90 nm design supported a single TE mode and could be patterned with photolithography, a relatively inexpensive technique offering high throughput. The sub-micron dimensions were chosen to provide anomalous dispersion for the TE mode through the waveguide geometrical contribution to dispersion. Additionally, the reduced effective mode area A_{eff} [7] led to larger nonlinear parameter $\gamma = 2\pi n_{2,wg}/(\lambda A_{eff})$, where λ is the wavelength, and $n_{2,wg}$ is the effective nonlinearity of the waveguide [8]. As shown in Fig. 1 [9], the 700 nm $\times$ 340 nm design supports one TE and one TM mode at 1.55 μm, which have A_{eff} of 0.2148 μm^2 and 0.3156 μm^2, respectively. Furthermore, these dimensions allow for tight bend radii of $\sim$3 μm with negligible calculated radiation loss and anomalous dispersion of -0.556 ps^2/m (TE mode). While the dispersion depends on exact waveguide dimensions [See Fig. 2(a)], using conservative fabrication tolerances, the targeted dispersion is expected to be within ± 0.18 ps^2/m.

To fabricate waveguides, a resist pattern is firs formed on a substrate, consisting of a 3 μm-thick oxide layer on top of a Si wafer. $Ge_{28}Sb_{12}Se_{60}$ is then thermally evaporated onto the patterned wafer, and lift-off is used to produce strip Ge-Sb-Se waveguides. Conventional photolithography was used to pattern the wider 2μm $\times$ 90 nm waveguides. The sub-micron waveguides were patterned with e-beam lithography, which offers improved resolutions of $\sim$ 10 nm and reduced sidewall roughness, compared with photolithography. To further improve the lift-off process, a bilayer resist composed of

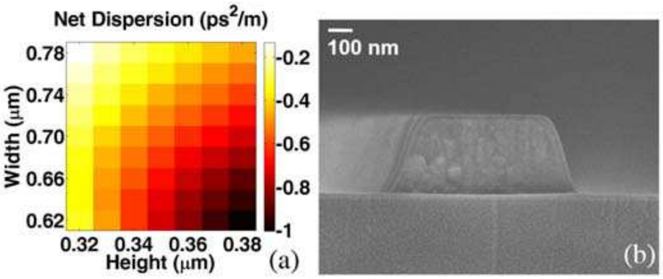

Fig. 2. (a) Simulated net dispersion (in ps^2/m) at 1550 nm for the TE mode of strip, air-clad $Ge_{28}Sb_{12}Se_{60}$ waveguides on a SiO_2 substrate for various core dimensions. (b) Scanning electron micrograph of a strip waveguide cross section, consisting of Si substrate (not pictured), 3-μm-thick SiO_2, a 700nm $\times$ 340 nm Ge-Sb-Se layer, and air upper cladding.

PMMA and PMMA-MMA copolymer was used [10,11]. Due to the difference in molecular weight, more of the underlying PMMA-MMA layer is removed than the PMMA overlayer, creating a slight overhang desired for subsequent lift-off.

III. Linear Optical Characterization

The linear absorption of bulk $Ge_{28}Sb_{12}Se_{60}$ (commercially available) was determined to be 0.07 ± 0.02 cm^{-1}, or 0.3 dB/cm, at a wavelength of 1.53μm from measurements of the incident, reflected and transmitted power at Brewster's angle, using a technique described by Ogusu et al. [12]. Corresponding measurements on a reference sample $Ge_{33}As_{12}Se_{55}$ agreed with values in literature [13].

Transmission measurements were performed on a 4.35μm-thick, thermally evaporated Ge-Sb-Se thin film From these measurements, the Tauc band edge was found to be 1.59$\pm$.01 eV, close to the 1.62 eV Tauc band edge of bulk $Ge_{28}Sb_{12}Se_{60}$ [3]. Energy Dispersive X-ray Spectroscopy measurements on thin Ge-Sb-Se film confirme that the stoichiometry of the fabricated thin film is within 4 atomic % of the bulk material [14]. A scanning electron micrograph (SEM) of a fabricated waveguide is shown in Fig. 2(b).

The top rms surface roughness was measured to be 0.8 nm using atomic force microscopy (AFM). Scanning electron microscopy was used to characterize the rms sidewall roughness, found to be $\sim$12 nm and 4 nm for the waveguides fabricated with photo- and e-beam lithography, respectively, as measured along the middle of the waveguide sidewall [15].

To characterize propagation loss, light at $\lambda = 1.53\mu$m was coupled into and out of the Ge-Sb-Se waveguides using high numerical aperture (NA = 0.35) fiber or tapered fiber mounted on piezo-actuated three-axis stages for precise alignment. Linearly polarized light was used to match the polarization of the desired guided mode. The intensity of the light scattered above the waveguide surface, I_{sc} was measured as a function of distance z along the waveguide using a cooled InGaAs detector array. Since I_{sc} is proportional to the intensity of the light remaining in the waveguide, a f t to a decaying exponential,$I_{sc} \propto \exp(-\alpha z)$ will yield the total loss α. Importantly, this method is not sensitive to variations in coupling loss. Measurements were made using low, 1-2 mW coupled cw power. To account for the intrinsic noise of the InGaAs camera, measurements without the laser were subtracted from those with the laser. Data from the firs $\sim$3 mm of the waveguide near the input facet was excluded from fitting due to non-negligible background from uncoupled light from the input fibe . We confirme that the InGaAs camera responded linearly for the experimental settings. We also checked that background light from slab-guided light was negligible by slightly misaligning the input fibe and verifying that no visible signal on the camera was produced.

TABLE I

Average Loss for Ge-Sb-Se Waveguides

Fabrication method	Fabrication parameters	Waveguide dimensions	Average TM loss (dB/cm)	Average TE loss (dB/cm)
Photolithography	NA	2000 nm x 90 nm	no TM mode	4.0±0.9
E-beam lithography	8 nA current, 8 nm grid	700 nm x 340 nm	5.6±1.0	6.1±0.8

Loss measurements were made on 3-5 adjacent waveguides for each fi ed waveguide dimensions and mode, and then averaged to obtain the loss, as summarized in Table 1. Given the low material absorption, propagation loss is dominated by scattering loss. The measured linear loss in our Ge-Sb-Se waveguides is similar to loss measured in other chalcogenide ($Ge_{23}Sb_7S_{70}$) strip waveguides of similar dimensions [16]. Although strip waveguides have higher loss than rib designs, we note that the strip geometry enables broader dispersion engineering and significantl reduced bend radii for resonator-enhanced nonlinear photonics.

IV. Nonlinear Optical Characterization

Loss in a waveguide due to both linear absorption and two-photon absorption is described by

$$\frac{1}{T} = \frac{[1 - e^{-\alpha L_{wg}}]\beta_{wg}}{\alpha} I + e^{\alpha L_{wg}}, \qquad (1)$$

where $1/T$ is the reciprocal transmission, I is the incident peak intensity, α is the linear absorption of the waveguide, β_{wg} is the two-photon absorption coefficien of the waveguide, and L_{wg} is the length of the waveguide [17].

The nonlinear loss of 700nm $\times$ 340 nm Ge-Sb-Se waveguides was determined through measurements of the output intensity as a function of input intensity. Vertically polarized, 170 fs-long pulses from a $\sim$1550 nm Er-doped fibe laser at a 17.8 MHz repetition rate were coupled into the TM mode of 10 mm-long waveguides. To verify the coupling loss, measurements were made launching light forwards through the waveguide, and then backwards, switching fibe patch cord connectors while leaving the tapered coupling fiber fi ed in position. Waveguides were illuminated with peak intensity up to 65 GW/cm^2 over 10 minutes. Data taken with increasing and decreasing power agreed and was repeatable. Figure 3 shows the reciprocal transmission vs. incident peak intensity. An average of fit to three data sets yields $\beta_{wg} = 0.014 \pm 0.003$ cm/GW for the TM mode of the waveguides. The main sources of error are the uncertainty in pulse shape and coupling efficien y, leading to uncertainty in the coupled peak power.

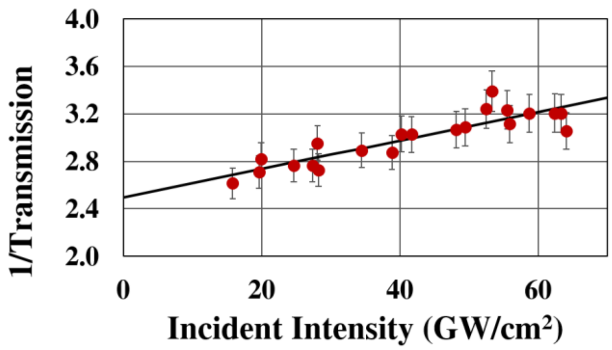

Fig. 3. Plot of reciprocal transmission as a function of incident peak intensity for the TM mode of the 700 nm by 340 nm Ge-Sb-Se waveguide. The average effective two-photon absorption coefficien is 0.014 ± 0.003 cm/GW.

Accounting for the band edge, wavelength, the fiel of the guided mode, and the waveguide materials, we fin that our measured value for β is in agreement with that predicted by the theory by Lenz et al. [18].

The input and output spectra from the 700nm $\times$ 340 nm Ge-Sb-Se waveguides were also measured, revealing a power-dependent broadening of the output spectral width, as measured at the -30 dB point. Simulations using the symmetrized split-step Fourier method [19] were employed to solve the scalar nonlinear Schrödinger equation, which included the effects of group velocity dispersion, higher order dispersion, linear and two-photon absorption, and self-phase modulation. The initial electric fiel amplitude and phase were determined using the PICASO phase retrieval algorithm using separate measurements of the spectrum and interferometric autocorrelation [20]. To determine $n_{2,wg}$ from the broadened spectra, measured parameters corresponding to the experimental setup, including α, β_{wg}, L_{wg}, the coupling efficien y, the input field and the simulated waveguide mode area A_{eff} [7] and dispersion (up to 4$^{\text{th}}$ order) were fi ed in the simulations, and $n_{2,wg}$ was used as a free parameter to fin a best fi to the experimentally measured spectral widths. A set of input and output spectra, along with corresponding simulation results, are shown in Fig. 4. While the simulations do not capture all the fin spectral features, they reproduce the general spectral shapes well. Averaging over three data sets, each including measurements on the TM mode taken at various coupled peak power levels from 60-140 W, we found $n_{2,wg} = 5 \pm 2 \times 10^{-19}$ m^2/W. This corresponds to a nonlinear parameter, $\gamma = 6 \pm 2$W^{-1}m^{-1} ($\sim$ 5000 $\times$ γ of single-mode SiO_2 fiber and a figur of merit, $FOM = (n_{2,wg}/\beta_{wg}\lambda)$ of 2.3 ± 0.9. The main sources of error in $n_{2,wg}$ are due to uncertainty in the initial pulse shape and temporal phase.

We acknowledge that our measurements of the waveguide nonlinearity are not time-resolved. Low throughput from the waveguides, primarily due to coupling loss, limits us from performing a pump-probe experiment with significantl weaker probe beam to study the time constant of the nonlinear response. These measurements are performed at wavelengths far from the band edge, where both linear and two-photon absorption are weak. This makes photosensitivity-induced

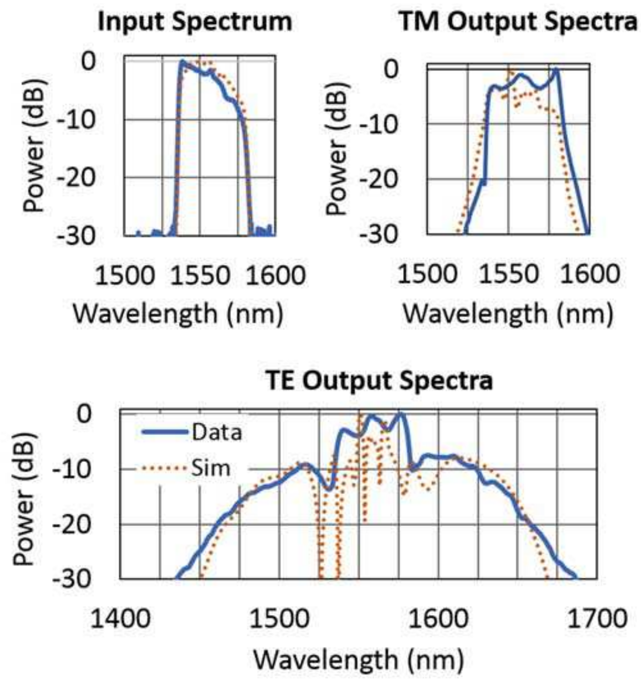

Fig. 4. Comparison of experimental data (solid blue line) and simulation (dashed orange line) of input and output spectra of the 10 mm-long, 700 nm by 340 nm Ge-Sb-Se waveguide, using coupled peak power of 87 W and 109 W for the TM and TE mode, respectively. The TE mode produces significantl more broadening than the TM mode due to its relatively low, anomalous dispersion of -0.556ps^2/m (vs. 6.23ps^2/m for TM).

changes less likely, though still possible, given observation of defect absorption-driven photosensitivity in other chalcogenides [21]. We also note that our measurements of the transmission were stable and reproducible, indicating the Ge-Sb-Se waveguides are photostable under these conditions.

The waveguide FOM is the same order-of-magnitude as FOM values measured on bulk samples of Ge-Sb-Se with slightly different composition, typically $\sim$1-8 at 1550 nm [4,18,22,23]. However, our values for $n_{2,wg}$ are roughly an order of magnitude lower than what is typically measured on bulk Ge-Sb-Se of similar composition [4,18,22,23]. Additionally, the predicted n_2 of 8.22×10^{-18}m^2/W for the material, calculated from Miller's Rule [4] using the linear refractive index of 2.66, is $\sim$ 14$\times$ larger than that measured in our waveguides, after accounting for a 0.867$\times$ enhancement factor from waveguide geometry for the TM mode [8]. While studies have shown that variations in composition can lead to changes in n_2 by $\sim$2-3 $\times$ [4,23], this cannot fully explain the large difference observed between bulk and waveguide. Some laser-written chalcogenide waveguides have been show to exhibit significantl lower n_2 than bulk [24], but reports of As_2S_3 and Ge-As-Se chalcogenide waveguides fabricated with lithography and etching show n_2 similar to bulk [25,26].

To further investigate, we performed similar nonlinear optical measurements using the TE mode of 2μm $\times$ 90 nm Ge-Sb-Se waveguides. We note these waveguides had $A_{eff} = 0.9241\mu$m^2, group velocity dispersion of 3.42ps^2/m, and a 1.12$\times$ enhancement factor from waveguide geometry [8]. For this set of waveguides, intensity-dependent transmission measurements revealed an average β_{wg} of 0.029 ± 0.007 cm/GW. Similarly, spectral broadening measurements indicated an average $n_{2,wg} = 8 \pm 2 \times 10^{-19}$ m^2/W, corresponding to $FOM = 1.8 \pm 0.7$. These values for the waveguides made using photolithography are the same order-of-magnitude as those for the waveguides fabricated using e-beam lithography. This suggests that the writing process alone is not fully responsible for relatively low nonlinearity compared to bulk. These two samples, in addition to having different patterning methods (photo- vs. e-beam lithography) are also from two different chalcogenide evaporations. This indicates the low nonlinearity compared to bulk is a relatively consistent issue. Additional study is required to better understand the source of our observed difference between waveguide and bulk. We are aware that this issue is a challenge for the broader chalcogenide community, probably not limited to our chosen material. Ellipsometry measurements have revealed a small difference in linear index between bulk and film and we are exploring possible ways to improve nonlinearity such as annealing. In spite of the lower nonlinearity observed in the waveguides, the measured FOM suggests that Ge-Sb-Se still holds promise as a nonlinear integrated optics platform at telecom wavelengths and beyond.

V. Conclusion

In summary, we fabricated single-mode, strip Ge-Sb-Se waveguides and characterized their optical properties at 1.53-1.55 μm. The linear loss, 4.0 dB/cm at the lowest, was dominated by scattering loss. The nonlinear loss of the waveguides fabricated with e-beam lithography was 0.014 ± 0.003 cm/GW, reasonable considering the wavelength and slight variations in band gap. Corresponding spectral broadening measurements revealed a nonlinear figur of merit of 2.3 ± 0.9 and nonlinear parameter of $6 \pm 2 \mathrm{W}^{-1}\mathrm{m}^{-1}$, indicating preliminary promise for nonlinear applications such as ultrafast switching at telecom wavelengths.

Acknowledgment

Part of this work was conducted at the Washington Nanofabrication Facility, a member of the NSF National Nanotechnology Infrastructure Network. We thank Richard Bojko (University of Washington) for technical discussions and e-beam lithography work, and Dr. Milos Popovic (Boston University) for use of his waveguide mode solver [9]. We also thank Suehyun Cho (University of Colorado Boulder) for SEM images, Dr. Thomas Murphy (University of Maryland) for his split-step software routine [18], and Caroline Hughes (University of Colorado Boulder) for measurement of bulk linear absorption.

References

[1] J. S. Sanghera *et al.*, "Non-linear properties of chalcogenide glasses and fibers" *J. Non-Cryst. Solids,* vol. 354, no. 2-9, pp. 462-467, Jan. 2008.

[2] B. J. Eggleton, B. Luther-Davies, and K. Richardson, "Chalcogenide photonics," *Nat. Photonics,* vol. 5, no. 3, pp. 141-148, Mar. 2011.

[3] P. Klocek and L. Columbo, "Index of refraction, dispersion, bandgap, and light in GeSe and GeSbSe glasses," *J. Non-Cryst. Solids*, vol. 93, no. 1, pp. 1-16, Aug. 1987.

[4] T. Wang *et al.*, "Systematic z-scan measurements of the third order nonlinearity of chalcogenide glasses," *Opt. Mater. Express*, vol. 4, no. 5, pp. 1011–1022, May 2014.

[5] J. Li *et al.*, "Sub-micrometer-thick and low-loss Ge20Sb15Se65 rib waveguides for nonlinear optical devices," *Optoelectron. Lett.*, vol. 11, no. 3, pp. 203-206, May 2015.

[6] W. Zhang *et al.*, "Rib and strip chalcogenide waveguides based on Ge-Sb-Se radio-frequency sputtered films" *Mat. Lett.*, vol. 98, pp. 42, 2013.

[7] G. P. Agrawal, *Nonlinear Fiber Optics,* 5th ed. Amsterdam: Academic Press, 2013, ch. *11*, sec. 1-*6*.

[8] S. Afshar V. and T. M. Monro, "A full vectorial model for pulse propagation in emerging waveguides with subwavelength structures part I: Kerr nonlinearity," *Opt. Express*, vol. 17, no. 4, pp. 2298-2318, 2009.

[9] M. Popovic, "Complex-frequency leaky mode computations using PML boundary layers for dielectric resonant structures," in *Integrated Photonics Research*, 2003, paper ITuD4.

[10] R. E. Howard *et al.*, "Multilevel resist for lithography below 100 nm," *IEEE Trans. on Electr. Dev.*, vol. 28, no. 11, pp. 1378-1381, Nov. 1981.

[11] A. A. Tseng *et al.*, "Electron beam lithography in nanoscale fabrication: recent development," *IEEE Trans. on Electron. Pack. Manufact.*, vol. 26, no. 2, pp. 141-149, Apr. 2003.

[12] K. Ogusu, K. Suzuki, and H. Nishio, "Simple and accurate measurement of the absorption coefficien of an absorbing plate by use of the Brewster angle," *Opt. Lett.*, vol. 31, no. 7, pp. 909-911, Apr. 2006.

[13] A. Prasad *et al.*, "Properties of $Ge_xAs_ySe_{1-x-y}$ glasses for all-optical signal processing," *Opt. Express*, vol. 16, no. 4, 2804-2815, Feb. 2008.

[14] M. R. Krogstad *et al.*, "Nonlinear characterization of $Ge_{28}Sb_{12}Se_{60}$ bulk and waveguide devices," *Opt. Exp.*, vol. 23, no. 6, pp. 7870-7878, 2015.

[15] M. R. Krogstad *et al.*, "Linear and nonlinear optical properties of Ge-Sb-Se waveguides at telecom wavelengths," in *CLEO*, 2016, paper SF1P.2.

[16] J. Hu *et al.*, "Si-CMOS-compatible lift-off fabrication of low-loss planar chalcogenide waveguides," *Opt. Express*, vol. 15, no. 19, pp. 11798-11807, Sept. 2007.

[17] T.-K. Liang and H.-K. Tsang, "Nonlinear absorption and raman scattering in silicon-on-insulator optical waveguides," *IEEE J. Sel. Topics in Quant. Electr.*, vol. 10, no. 5, pp. 1149-1153, Sept.-Oct. 2004.

[18] G. Lenz *et al.*, "Large Kerr effect in bulk Se-based chalcogenide glasses," *Opt. Lett.*, vol. 25, no. 4, pp. 254-256, Feb. 2000.

[19] T. M. Murphy, "SSPROP," Available: http://www.photonics.umd.edu /software/ssprop/ [23 November 2015].

[20] J. W. Nicholson and W. Rudolph, "Noise sensitivity and accuracy of femtosecond pulse retrieval by phase and intensity from correlation and spectrum only (PICASO)," *J. Opt. Soc. Am. B,* vol. 19, no. 2, pp. 330-339, Feb. 2002.

[21] J. Hu *et al.*, "Resonant cavity-enhanced photosensitivity in As2S3 chalcogenide glass at 1550 nm telecommunication wavelength," *Opt. Lett.*, vol. 35, no. 6, pp. 874-876, Mar. 2010.

[22] S. Dai *et al.*, "Mid-infrared optical nonlinearities of chalcogenide glasses in Ge-Sb-Se ternary system," *Opt. Exp.*, vol. 23, no. 2, pp. 1300-1307, Jan. 2015.

[23] M. Olivier *et al.*, "Structure, nonlinear properties, and photosensitivity of $(GeSe_2)_{100-x}(Sb_2Se_3)_x$ glasses," *Opt. Mater. Express*, vol. 4, no. 3, pp. 525-540, Mar. 2014.

[24] J. E. McCarthy *et al.*, "Mid-infrared spectral broadening in an ultrafast laser inscribed gallium lanthanum sulphide waveguide," *Opt. Express*, vol. 20, no. 2, pp. 1545-1551, Jan. 2012.

[25] S. J. Madden *et al.*, "Long, low loss etched As_2S_3 chalcogenide waveguides for all-optical signal regeneration," *Opt. Express*, vol. 15, no. 22, pp. 14414-14421, Oct. 2007.

[26] X. Gai *et al.*, "Dispersion engineered $Ge_{11.5}As_{24}Se_{64.5}$ nanowires with a nonlinear parameter of $136\mathrm{W}^{-1}\mathrm{m}^{-1}$ at 1550nm," *Opt. Express*, vol. 18, no. 18, pp. 18866–18874, Aug. 2010.